Evidence of Natural Selection Acting on a Polymorphic Hybrid Incompatibility Locus in *Mimulus*

Andrea L. Sweigart*,[1] and Lex E. Flagel[†,‡,2]

*Department of Genetics, University of Georgia, Athens, Georgia 30602, [†]Department of Biology, Duke University, Durham, North Carolina 27708, and [‡]Department of Plant Biology, University of Minnesota, St. Paul, Minnesota 55108

ABSTRACT As a common cause of reproductive isolation in diverse taxa, hybrid incompatibilities are fundamentally important to speciation. A key question is which evolutionary forces drive the initial substitutions within species that lead to hybrid dysfunction. Previously, we discovered a simple genetic incompatibility that causes nearly complete male sterility and partial female sterility in hybrids between the two closely related yellow monkeyflower species *Mimulus guttatus* and *M. nasutus*. In this report, we fine map the two major incompatibility loci—*hybrid male sterility 1* (*hms1*) and *hybrid male sterility 2* (*hms2*)—to small nuclear genomic regions (each <70 kb) that include strong candidate genes. With this improved genetic resolution, we also investigate the evolutionary dynamics of *hms1* in a natural population of *M. guttatus* known to be polymorphic at this locus. Using classical genetic crosses and population genomics, we show that a 320-kb region containing the *hms1* incompatibility allele has risen to intermediate frequency in this population by strong natural selection. This finding provides direct evidence that natural selection within plant species can lead to hybrid dysfunction between species.

KEYWORDS speciation; hybrid incompatibilities; postzygotic reproductive isolation; *Mimulus*; monkeyflower

SPECIATION occurs when diverging populations accumulate genetic differences that cause reproductive isolation. Many forms of prezygotic reproductive isolation likely evolve as byproducts of adaptation to different ecological conditions (*e.g.*, habitat or behavioral differences), but the evolutionary dynamics of intrinsic postzygotic isolation are less clear. This is because the production of dead or sterile hybrids cannot be favored by natural selection. Dobzhansky (1937) and Muller (1942) proposed a solution to this long-standing mystery (Darwin 1859), explaining that a new mutation might function perfectly well with alleles present in its native species, and only cause sterility or inviability when found in a hybrid genetic background. The so-called Dobzhansky–Muller model shows that natural selection need not oppose the evolution of hybrid dysfunction, but it makes no predictions about the nature of the genetic changes or the evolutionary forces that give rise to hybrid incompatibilities.

doi: 10.1534/genetics.114.171819
Manuscript received October 13, 2014; accepted for publication November 18, 2014; published Early Online November 25, 2014.
Supporting information is available online at http://www.genetics.org/lookup/suppl/doi:10.1534/genetics.114.171819/-/DC1.
[1]Corresponding author: Department of Genetics, 120 East Green St., Davison Life Sciences Building, University of Georgia, Athens, GA 30602.
E-mail: sweigart@uga.edu
[2]Present address: Monsanto Company, Chesterfield, MO 63017.

The recent identification of several hybrid incompatibility genes in diverse taxa has begun to reveal some insights into the evolution of hybrid dysfunction (reviewed in Presgraves 2010; Maheshwari and Barbash 2011; Sweigart and Willis 2012). In *Arabidopsis* and rice, genetic incompatibilities have been mapped to duplicate genes that carry loss-of-function alleles in alternate copies (Bikard *et al.* 2009; Mizuta *et al.* 2010; Yamagata *et al.* 2010), suggesting that divergence among paralogs via mutation and genetic drift might cause postzygotic reproductive isolation (Lynch and Force 2000). There are also hints that natural selection can contribute to the spread of incompatible alleles within populations and species. For example, plant hybrid necrosis has been mapped repeatedly to disease resistance genes (Krüger *et al.* 2002; Bomblies *et al.* 2007; Alcazar *et al.* 2009; Jeuken *et al.* 2009; Yamamoto *et al.* 2010; Chen *et al.* 2014), which are likely targets of adaptive divergence to unique pathogen communities (Bomblies and Weigel 2007). Additionally, many hybrid incompatibility genes show molecular signatures of positive selection (Presgraves *et al.* 2003; Brideau *et al.* 2006; Maheshwari *et al.* 2008; Oliver *et al.* 2009; Phadnis and Orr 2009; Tang and Presgraves 2009), but, interestingly, few of these genes seem to be involved in classical ecological adaptation. Instead, it has been proposed that rapid divergence at hybrid incompatibility loci might be driven by recurrent bouts

of intragenomic conflict involving segregation distorters (Frank 1990; Hurst and Pomiankowski 1991). Consistent with this idea, studies in *Drosophila* and rice find that hybrid segregation distortion maps to the same genomic locations as hybrid sterility (Tao *et al.* 2001; Long *et al.* 2008; Phadnis and Orr 2009; Zhao *et al.* 2010; Yang *et al.* 2012). Ultimately, an important challenge for speciation geneticists is to determine which evolutionary forces cause the *initial* spread of incompatibility alleles within species.

A promising way forward is to focus on young species pairs that are not yet fixed for hybrid incompatibilities. There is now abundant evidence from diverse systems that polymorphic loci contribute to variation in hybrid dysfunction (Cutter 2012); in some cases, it is feasible to both genetically map hybrid incompatibilities and investigate their evolutionary dynamics in natural populations. This combination of approaches was used in a recent study of *Mimulus guttatus*, which showed that a hybrid lethality allele at the *NecI* locus hitchhiked to high frequency during the adaptive fixation of a copper tolerance allele at a tightly linked gene (Wright *et al.* 2013). Additional studies of this sort are needed to determine which population genetic forces and selective agents are most important for the evolution of postzygotic reproductive isolation.

Here we investigate the genetics and evolution of a well-characterized hybrid incompatibility between two closely related species of monkeyflower, *M. guttatus* and *M. nasutus*. In this system, two major incompatibility loci—*hybrid male sterility 1* (*hms1*) and *hybrid male sterility 2* (*hms2*)—cause nearly complete male sterility and partial female sterility in *Mimulus* hybrids (Sweigart *et al.* 2006). Additionally, we know how these loci vary in nature: the *hms1* incompatibility allele has a limited distribution in *M. guttatus* and is even polymorphic within populations, whereas the *hms2* incompatibility allele is geographically widespread, and potentially fixed, in *M. nasutus* (Sweigart *et al.* 2007). This genetically simple, polymorphic hybrid incompatibility system in a young species pair sets the stage to directly link the intraspecific causes of divergence to hybrid dysfunction.

In the present study, we perform fine-scale genetic mapping to narrow the *hms1* and *hms2* intervals. In both genomic regions, we identify strong candidate genes for *Mimulus* hybrid sterility. We also take advantage of natural variation within *M. guttatus* to investigate the evolutionary dynamics of *hms1*. Using a population genomics approach, we discover that strong natural selection has driven the *hms1* incompatibility allele to intermediate frequency within a population of *M. guttatus*. This study provides an especially detailed look at the evolution of a hybrid incompatibility locus that is still in the early stages of divergence.

Materials and Methods

Study system

The *M. guttatus* species complex is a group of closely related, phenotypically diverse wildflowers that exhibits tremendous variation in reproductive isolation between populations and species. Our study focuses on the most geographically widespread and morphologically extreme members of the complex: *M. guttatus*, an outcrosser with large, bee-pollinated flowers, and *M. nasutus*, a selfer with reduced, mostly closed flowers. Despite their phenotypic differences, these species are closely related, having diverged ~200,000 years ago (Brandvain *et al.* 2014). Natural populations of both species are abundant throughout much of western North America but the range of *M. nasutus* is more restricted. In areas of overlap, the two *Mimulus* species are partially reproductively isolated by differences in floral morphology, flowering phenology, and pollen–pistil interactions (Diaz and MacNair 1999; Martin and Willis 2007; Fishman *et al.* 2014). Nevertheless, hybrids are frequently observed at sympatric sites (Vickery 1964; Martin and Willis 2007; A. M. Kenney and A. L. Sweigart, unpublished results), and we find evidence of genome-wide introgression (Sweigart and Willis 2003; Brandvain *et al.* 2014). Hybrid incompatibilities are also common, but variable (Vickery 1978; Christie and MacNair 1987; Sweigart *et al.* 2007; Case and Willis 2008; Martin and Willis 2010).

Specific lines and previous genetic mapping

Previously, we identified a pair of nuclear incompatibility loci that causes nearly complete male sterility and partial female sterility in a fraction of F_2 hybrids between an inbred line of *M. guttatus* from Iron Mountain, Oregon (IM62), and an *M. nasutus* line from Sherar's Falls, Oregon (SF5) (Sweigart *et al.* 2006). The incompatibility is between a semidominant IM62 allele at *hms1* and recessive SF5 alleles at *hms2*. Initially, we mapped *hms1* to a region of 12 cM on linkage group 6 and *hms2* to 8 cM on linkage group 13 (Sweigart *et al.* 2006). Following the release of the *M. guttatus* reference genome (generated from the IM62 line, www.phytozome.net), we identified previously unmapped, gene-based MgSTS markers (http://www.mimulusevolution.org) in these intervals. We also designed new, intron-spanning, length-polymorphic markers targeted to each locus. Using F_2 recombinants generated in our previous study and these new markers, we refined each hybrid sterility locus: *hms1* was mapped between flanking markers M8 and M24, and *hms2* between MgSTS193 and M51 (primer sequences for these markers are in Supporting Information, Table S1).

Fine mapping

To fine map *hms1* and *hms2*, we generated two large SF5 × IM62 F_2 mapping populations in consecutive years (in 2011, $N = 4220$ and in 2012, $N = 4894$). The first F_2 population was grown in the greenhouse at the University of Montana (in 2011) and the second at the University of Georgia (in 2012). Seeds were planted into 96-well flats containing Fafard 3b potting mix, chilled for 7 days at 4° to promote germination, and then placed in a greenhouse with supplemental lights set to 16-hr days. Plants were bottom watered daily and temperatures were maintained at 24° during the day and 16° at night.

We collected leaf tissue from all F_2 hybrids and isolated genomic DNA using a rapid extraction protocol (Cheung *et al.* 1993) modified for 96-well format. We then genotyped these F_2 hybrids for a multiplexed set of fluorescently labeled markers that flank *hms1* (M8 and M24) and *hms2* (MgSTS193 and M51) following amplification protocols used previously (Sweigart *et al.* 2006, 2007). All individuals with informative recombination events in either interval were retained and genotyped at additional markers designed by walking through the *hms1* and *hms2* regions of the IM62 *M. guttatus* genome sequence assembly. Publically available resequence data from the SF5 *M. nasutus* parent (Table S2) allowed us to develop new markers that span known SNPs and/or indel polymorphisms (Table S1). All genotypes were scored automatically using GeneMarker (SoftGenetics), with additional hand scoring where necessary. Male fertility (*i.e.*, pollen viability) for informative recombinants was assessed as described previously (Sweigart *et al.* 2006, 2007).

To map *hms1*, we retained individuals that were homozygous for SF5 alleles at both *hms2* flanking markers and recombinant for *hms1* markers. Because these individuals are homozygous for the SF5 incompatibility allele at *hms2*, they will be male sterile if they also carry at least one IM62 allele at the causal *hms1* locus. For one class of *hms1* recombinants—those that are homozygous for SF5 alleles at one flanking marker and heterozygous at the other—it is straightforward to assess the effect of genotype on male fertility phenotype. However, for the other class of *hms1* recombinants—those that are homozygous for IM62 alleles at one marker and heterozygous at the other—progeny testing is required (this is because there is no phenotypic variation among this class of recombinants; all are highly male sterile, having inherited at least one copy of the IM62 allele). We used these male sterile F_2 recombinants as maternal parents in crosses to SF5: individuals that are homozygous for IM62 alleles at *hms1* produce only male sterile progeny (all are heterozygous at *hms1* and homozygous for SF5 alleles at *hms2*), and those that are heterozygous at *hms1* produce progeny that segregate 1:1 for male fertility.

To map *hms2*, we identified individuals from the 2011 F_2 mapping population that carried at least one IM62 allele at *hms1* (heterozygous or homozygous for IM62 alleles at *hms1* flanking markers) and were recombinant for *hms2* markers. For *hms2*, we retained only one class of recombinants—those homozygous for SF5 alleles at one *hms2* marker and heterozygous at the other. Because these F_2 recombinants all carry at least one IM62 allele at *hms1*, they are expected to be male sterile if they are homozygous for SF5 alleles at *hms2* and male fertile if they are heterozygous. However, male fertility among these *hms2* recombinants is not entirely discrete, due to both incomplete dominance at *hms1* and variation at additional, small-effect hybrid sterility loci (see figure 5 in Sweigart *et al.* 2006). To address this issue, we used a QTL mapping approach to localize hybrid sterility effects in the *hms2* region. Linkage analysis was performed using JoinMap 4.1 (Van Ooijen 2006) by genotyping a subset of informative recombinants for *hms2*. To preserve realistic genetic distances, we also included nonrecombinant F_2 genotypes (*i.e.*, individuals with the same genotype at both *hms2*-flanking markers) in the linkage analysis and assumed no recombination among intervening markers. A genetic map was constructed using the maximum likelihood mapping algorithm and Haldane mapping function. Markers were given a fixed order (based on physical locations) and grouped with a LOD score threshold of 10.0. To detect QTL, we used the R/qtl package (Broman *et al.* 2003) to run a "scanone" analysis in 1-cM steps using the Haley–Knott regression.

For a subset of *hms1* and *hms2* recombinants, we performed additional progeny testing to improve our confidence in phenotypic assignments (Table S3 and Table S4). The idea was to minimize variation in hybrid male fertility due to the environment (*e.g.*, common greenhouse pests like thrips can lower pollen viability). To generate progeny, fertile recombinants were self-fertilized and male sterile recombinants were crossed to SF5 (using the F_2 hybrid as the maternal parent). For 10 *hms1* recombinants and 12 *hms2* recombinants, we scored between 10 and 106 progeny for *hms1-2* genotypes and male fertility phenotypes (an average of 43 progeny were measured).

Crosses to detect carriers of the hms1 incompatibility allele

Previously, we showed that *hms1* is polymorphic within the Iron Mountain population and that the hybrid sterility allele occurs at intermediate frequency (Sweigart *et al.* 2007). To test for the presence of *hms1* incompatibility alleles in additional *M. guttatus* inbred lines derived from the IM population, we performed backcrosses between them and SF5. If a particular IM inbred line carries an IM62-like hybrid sterility allele at *hms1*, roughly one-fourth of its progeny in an F_1 backcross to SF5 is expected to have the incompatible genotype. If instead, the IM inbred line carries a compatible allele at *hms1*, genotypes at *hms1* and *hms2* should not affect male fertility. For each IM inbred line-SF5 backcross, we measured pollen viability and determined *hms1* and *hms2* genotypes for at least 24 progeny (an average of 42 were measured). We then performed an ANOVA for each cross to assess the contribution of *hms1* and *hms2* to variation in hybrid male fertility.

Sequencing and population genomic analyses

To examine population genomic variation for *hms1* and *hms2*, we used whole genome resequence data from 10 IM inbred lines (Flagel *et al.* 2014) and 10 *M. guttatus* complex accessions sampled from throughout the species range (Table S2; for accession information see Brandvain *et al.* 2014). For the IM inbred lines, full protocols for genomic DNA isolation, Illumina sequencing, and sequence alignment can be found in Flagel *et al.* 2014. Briefly, each line was sequenced to ~7–15 times the genomic coverage using Illumina paired-end sequences. These sequences were aligned to the IM62 v2.0 reference genome assembly (ftp://ftp.jgi-psf.org/pub/compgen/phytozome/v9.0/early_release/Mguttatus_v2.0/assembly/)

using the Burrows-Wheeler Aligner (Li and Durbin 2010). We then performed base calls using the *UnifiedGenotyper* method in GATK v3.2 (Depristo *et al.* 2011). We retained sites with a genotype quality score of ≥30. Raw sequence data can be found at the National Center for Biotechnology Information Sequence Read Archive accessions listed in Table S2. For population genomic analyses, we fit an integrated *Mimulus* genetic map (described in Brandvain *et al.* 2014) to physical positions from the IM62 sequence assembly.

Because we resequenced the inbred line used to create the reference genome (IM62) we have a direct estimate of the sequencing/genotyping error rate for our samples. Genome-wide, the difference between genotype calls for the resequenced IM62 and the IM62 reference genome was 2.6 SNPs every 10 kb (*i.e.*, total $\pi_{error} = 2.6 \times 10^{-4}$). Assuming half the errors belong to the reference and half belong to our method, we can estimate our lower detection limit for diversity to be approximately $\pi = 1.3 \times 10^{-4}$.

To design genetic markers that distinguish *hms1* haplotype groups (see *Results*), we screened for SNP differences that create polymorphic restriction sites. These cleaved amplified polymorphic sequence (CAPS) markers (Table S1) were used to examine *hms1* genomic variation in a large collection of inbred lines derived from the IM population.

Results

Fine mapping localizes hybrid sterility to strong candidate genes

To fine map *Mimulus* hybrid sterility loci, we genotyped all individuals from two large F_2 mapping populations at gene-based markers (see www.mimulusevolution.org and Table S1) known to flank *hms1* (M8 and M24) and *hms2* (M51 and MgSTS193). Consistent with previous findings (Sweigart *et al.* 2006), we observed significant transmission ratio distortion at *hms2* with a deficit of *M. nasutus* alleles (frequency of *M. guttatus* to *M. nasutus* alleles: expected = 0.5:0.5, observed = 0.62:0.38, $\chi^2 = 177.14$, d.f. = 1, $P < 0.0001$, $N = 6137$). At *hms1*, allelic transmission did not differ from the Mendelian expectation (*M. guttatus* to *M. nasutus* alleles: expected = 0.5:0.5, observed = 0.49:0.51, $\chi^2 = 0.44$, d.f. = 1, $P = 0.51$, $N = 7028$).

To dissect the *hms1* locus, we focused on a small subset of F_2 hybrids that were both recombinant at *hms1* and homozygous for *M. nasutus* alleles at *hms2* (note that this *hms2* genotypic class is small due to the transmission ratio distortion reported above). We then genotyped these recombinants at additional markers targeted to the *hms1* region. As shown in Figure 1, F_2 recombination within this region localizes the *hms1* sterility effects to an interval of only 67,893 bp with 11 predicted genes (Table 1).

The genes that map to the *hms1* locus include three strong candidates for involvement in hybrid sterility. *Migut.F01605* and *Migut.F01606* are tandem duplicates of *SKP1*-like genes. In *Arabidopsis*, *SKP1* (*ASK1*) mutants cause male sterility and the *SKP1* gene functions during meiosis (Yang *et al.* 1999). *Migut.F01612* is annotated as a member of the *F-box* gene family, which mediates protein–protein interactions and influences diverse developmental traits including fertility (*e.g.*, Devoto *et al.* 2002; Kim *et al.* 2010). Intriguingly, of the few hybrid sterility genes cloned in rice, one encodes an F-box gene (*Sa*, Long *et al.* 2008). Although none of the other *hms1*-interval genes have such clear connections to gametogenesis, we cannot yet rule out their involvement in *Mimulus* hybrid sterility. Indeed, two of the predicted genes in the *hms1* interval (*Migut.F01610* and *Migut.F01611*) are members of large gene families that play a variety of roles during plant development. Two others lack functional annotations altogether, so it is unclear how they might affect fertility. Going forward, additional rounds of fine mapping and/or functional experiments will be needed to identify which of these *hms1* genes causes *Mimulus* hybrid sterility.

To fine map *hms2*, we identified F_2 hybrids that were recombinant at *hms2* and also carried at least one *M. guttatus* allele at *hms1*. Against this *hms1* background, which is carried by roughly three-quarters of the F_2 hybrids, we identified a large number of informative recombinants in the 2011 F_2 mapping population ($N = 130$ recombinants homozygous for *M. nasutus* alleles at one *hms2* flanking marker and heterozygous at the other). To narrow the genomic region associated with hybrid male sterility, we took a QTL mapping approach, genotyping the *hms2* recombinants for newly designed markers spanning the region between the original flanking markers MgSTS193 and M51. The QTL for hybrid male sterility is highly significant [likelihood ratio (LR) = 17.8 *vs.* an LR threshold of 1.65; Figure 2] and maps to a 98,503-bp interval between markers M216 and M211 (1 LOD-drop boundaries). Further progeny testing for 12 of the *hms2* recombinants suggests that the QTL resides in a region of only 60,052 bp containing five predicted genes (Table 1). One of these, *Migut.M00294*, is annotated as a cdc2-related protein kinase and is a strong candidate for *hms2*. Highly conserved among all eukaryotes, cdc2 is a key regulator of the cell cycle. In *Arabidopsis*, a loss-of-function mutation in a homolog of cdc2 (*CDKA; 1*) results in pollen lethality due to a failure of generative cell division in male gametogenesis (Nowack *et al.* 2005; Iwakawa *et al.* 2006). Although the other four candidate genes in the *hms2* region have no known roles in pollen development, as with *hms1*, additional experiments are needed to determine with certainty which gene underlies *hms2*.

The hms1 sterility allele is at intermediate frequency within the Iron Mountain population

To examine natural variation for *hms1* within the Iron Mountain population of *M. guttatus*, we tested for the presence of the incompatibility allele in 18 inbred lines derived from this locale. Consistent with our previous results (Sweigart *et al.* 2007), we find that the *hms1* incompatibility allele is at intermediate frequency in the Iron Mountain population: 9 of the 18 IM inbred lines segregate male sterile progeny when backcrossed to SF5 and variation in male fertility is strongly

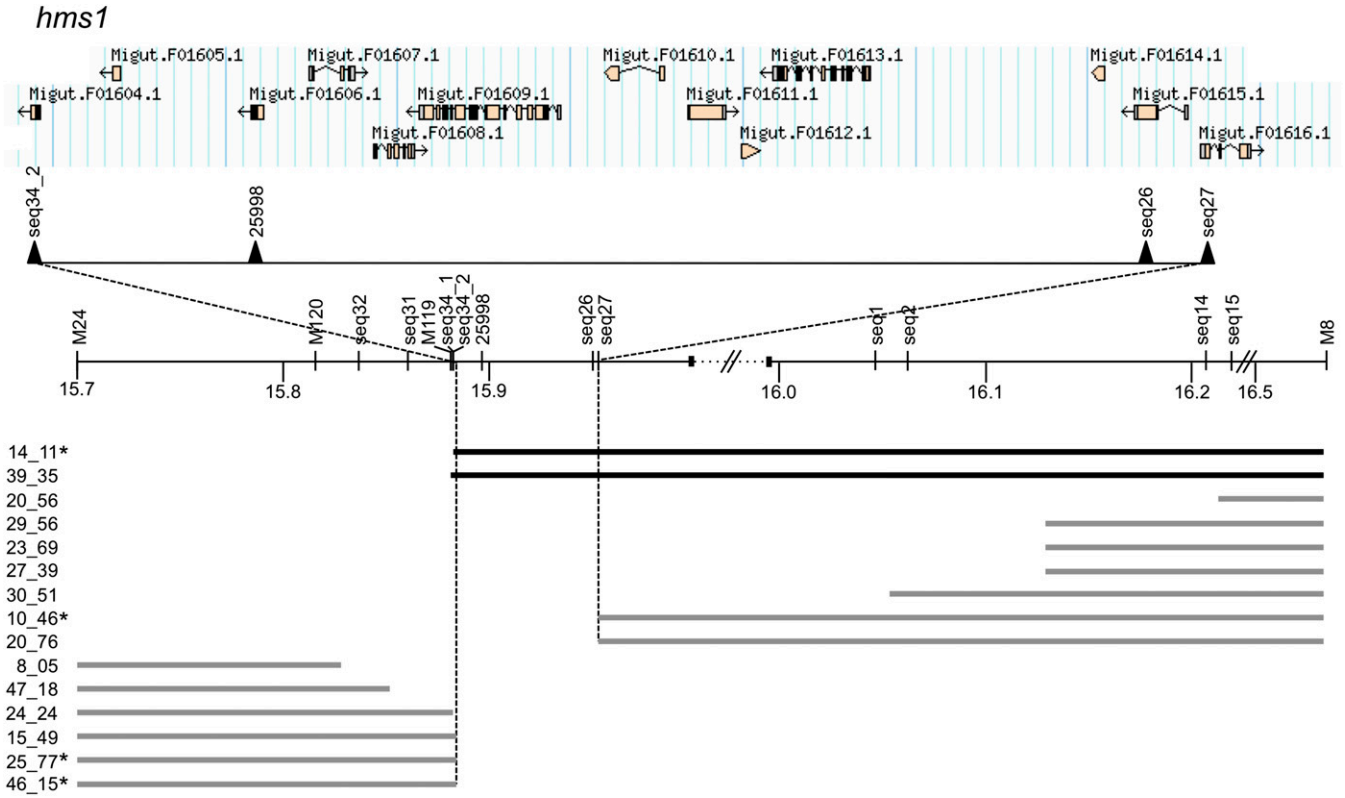

Figure 1 Genetic dissection and physical map of the *hms1* locus in *Mimulus*. Informative recombinants from an F_2 mapping population are shown with horizontal bars representing heterozygous genotypes, or, for recombinants that required progeny testing (indicated by asterisks), regions homozygous for *M. guttatus* alleles (see *Materials and Methods* for details). Solid bars indicate male-sterile individuals and shaded bars indicate male-fertile individuals. Physical locations of genetic markers (1 Mb shown) map hybrid male sterility to a region of only 68 kb (between markers seq34_2 and seq27) that includes 11 predicted genes. Annotation is based on *M. guttatus* Annotation v2.0, phytozome.net (*M. guttatus* v1.1 assembly scaffolds are separated by dotted lines with double hash marks).

associated with *hms1* inheritance (Table 2). The other 9 IM lines produce mostly fertile progeny when backcrossed to SF5 and show no effect of genotype at the *hms1* locus. Although our sample sizes were often too small to detect a significant interaction between *hms1* and *hms2*, the backcross progeny that carried the *hms1-hms2* incompatibility (*i.e.*, heterozygous at *hms1* and homozygous for *M. nasutus* alleles at *hms2*) were almost always the most sterile genotype.

Evidence for a selective sweep at hms1

Using whole genome resequence data from 10 IM inbred lines (including IM62), we discovered an intriguing pattern of population genomic variation within and around *hms1*. Among this sample of lines, five carry a nearly invariant haplotype that extends for 320 kb and includes the *hms1* locus (group 1, Figure 3A; π in the 320-kb region = 9.7×10^{-5}). In this same genomic region, the other five IM lines show typical levels of nucleotide variation (group 2, Figure 3A; π in the 320-kb region = 0.016, among all IM lines π genome-wide = 0.014). Moreover, the group 1 IM haplotype does not appear to be a common variant throughout the species' range: in this 320-kb region, group 1 and group 2 IM lines are similarly divergent from a sample of several *M. guttatus* complex lines (including SF5) collected from diverse locales (see Table S2; π in the 320-kb region: group 1 *vs. M. guttatus* complex = 0.026, group 2 *vs. M. guttatus* complex = 0.024). Note that although the sharp "borders" of the 320-kb haplotype might seem to suggest an inversion, this possibility is inconsistent with our earlier finding of several SF5 × IM62 F_2 hybrid *hms1* recombinants within this same interval, which indicate this region is collinear (see Figure 1).

Using *hms1*-linked genomic sequence from these 10 IM lines, we designed two CAPS markers (Table S1) targeted to the outside edges of the 320-kb region that were diagnostic for haplotype group in this sample. We then used these CAPS markers to genotype a large panel of inbred lines from Iron Mountain. In this larger sample, the group 1 haplotype segregates at intermediate frequency (44%, N = 126 individuals).

To determine whether or not polymorphism for male sterility at *hms1* is associated with variation at this 320-kb haplotype, we focused on the 18 IM inbred lines with known *hms1* phenotypes (Table 2). Among this sample, allelic status at *hms1* is highly predictive of haplotype group. Of the 9 IM inbred lines that carry the hybrid sterility allele at *hms1*, 8 carry the group 1 haplotype and only 1 line carries a group 2 sequence. The opposite pattern is seen for the 9 IM inbred lines that carry a compatible allele at *hms1*: 8 of these lines carry group 2 haplotypes and only 1 line carries a group 1

Table 1 Predicted genes found in fine mapped regions of *hms1* and *hms2*

Locus	Gene name[a]	Gene annotation[a]	Predicted functional role[b]	Sterility phenotype in *Arabidopsis*?
hms1	Migut.F01605 and Migut.F01606	Skp1 family	Cell cycle regulation, component of SCF ubiquitin–ligase complex[c]	*Arabidopsis Skp1* homolog (*ASK1*) mutant causes male sterility via defects in male meiosis[d]
	Migut.F01607	Iron–sulfur cluster biosynthesis	Iron–sulfur cluster binding, structural molecule activity	
	Migut.F01608	4′-phosphopantetheinyl transferase superfamily	Involved in metabolic processes, macromolecule biosynthesis	
	Migut.F01609	None		
	Migut.F01610	Leucine rich repeat (LRR)	Kinase activity, signal transduction; diverse roles in plant development and disease resistance[e]	Mutations in *EMS1/EXS* (1 of >200 LRR genes in *Arabidopsis*) causes male sterility when microsporocytes do not undergo proper cytokinesis[f]
	Migut.F01611	PPR repeat	Organellar RNA processing, embryonic development[g]	Some members of this large gene family (450 in *Arabidopsis*) are involved in fertility restoration of CMS plants[h]
	Migut.F01612	F-box	Component of SCF ubiquitin–ligase complex, targets specific proteins for degradation	Among this large gene family (>600 in *Arabidopsis*), *COI1* mutants are male sterile[i], *FBL17* mutants inhibit male germline proliferation[j], the rice hybrid sterility gene *SaF* encodes an F-box protein[k]
	Migut.F01613	None		
	Migut.F01614	Yip1 domain; Golgi membrane protein	Involved in the *trans*-Golgi network[l]	
	Migut.F01615	Amino acid kinase family; gamma-glutamyl kinase	Amino acid biosynthesis	
hms2	Migut.M00294	Protein kinase domain; cdc2-related protein kinase	Cyclin-dependent kinase (CDK)-like protein[m], cell cycle regulation	*Arabidopsis* cdc2 mutant (*CDKA;1*) is male sterile because it fails to progress through the second mitosis in male gametogenesis[n]
	Migut.M00295	Cellulase (glycosyl hydrolase family 5)	Involved in carbohydrate metabolism, hydrolase activity	
	Migut.M00296	None		
	Migut.M00297	RNA polymerase Rpb2	Encodes a subunit of DNA-dependent RNA polymerase II	
	Migut.M00298	GH3 auxin-responsive promoter	Involved in red light-specific hypocotyl elongation	

[a] http://www.phytozome.net.
[b] Unless a citation is provided, functional descriptions are taken from TAIR (arabidopsis.org) for the gene's closest *Arabidopsis thaliana* BLAST hit.
[c] Bai *et al.* 1996; Yang *et al.* 2012.
[d] Yang *et al.* 1999.
[e] Diévart and Clark 2004.
[f] Canales *et al.* 2002; Zhao *et al.* 2002.
[g] Saha *et al.* 2007.
[h] Barr and Fishman 2010; Barkan and Small 2014.
[i] Xie *et al.* 1999.
[j] Kim *et al.* 2008; Gusti *et al.* 2009.
[k] Long *et al.* 2008.
[l] Drakakaki *et al.* 2012.
[m] Menges *et al.* 2005.
[n] Nowack *et al.* 2005; Iwakawa *et al.* 2006.

haplotype. This association between *hms1* haplotype and hybrid sterility phenotype in these 18 IM inbred lines is highly significant (Fisher's exact test, $P = 0.0034$). Note that the two exceptions to the general pattern (IM232 and IM591) are IM lines that show somewhat atypical hybrid sterility, which might be caused by environmental and/or genetic background effects. Of all the IM inbred lines that were identified as carriers of the hybrid sterility allele at *hms1* (Table 2), IM232 is the only one for which the *hms1-hms2* incompatibility genotype (*i.e.*, heterozygous at *hms1* and homozygous for *M. nasutus* alleles at *hms2*) is not the most sterile genotypic class. Additionally, among the lines identified as carrying compatible alleles at *hms1*, IM591 shows fairly high backcross sterility and a modest (nonsignificant) effect of *hms1* genotype. Taken together, these results provide strong evidence that the *hms1* sterility

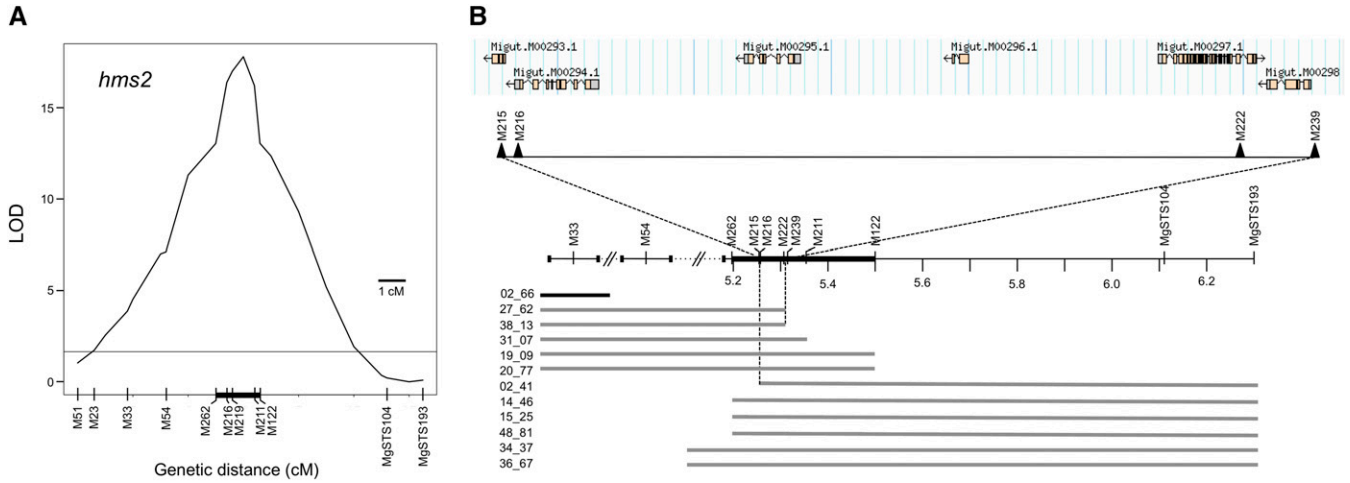

Figure 2 Genetic dissection and physical map of the *hms2* locus in *Mimulus*. (A) QTL profile generated from informative *hms2* F_2 recombinants that also carry at least one *M. guttatus* allele at *hms1*. The positions of molecular markers are indicated along the bottom. Hybrid male sterility effects were mapped to an interval of roughly 1 cM between M216 and M211. The thick black bar along the *x*-axis indicates a 2-LOD drop on either side of the peak, corresponding to 1.6 cM. The horizontal line at 1.65 shows the 5% significance LOD threshold generated using 1000 permutations. (B) Progeny testing for a subset of the informative *hms2* recombinants further refined the sterility locus. The *hms2* F_2 recombinants are shown with horizontal bars representing heterozygous genotypes (regions left blank indicate markers homozygous for *M. nasutus* alleles). Because all of these individuals carry at least one *M. guttatus* allele at *hms1*, they are sterile if they are also homozygous for *M. nasutus* alleles at *hms2*. Black bar indicates a male-sterile individual and shaded bars indicate male-fertile individuals. (Note that the larger number of male fertiles reflects a bias in seed production between these phenotypic classes; we were more likely to collect seeds from male-fertile recombinants.) Physical locations of genetic markers (~1 Mb shown) map hms2 to a region of only 60,052 bp (between markers M215 and M239) that includes five predicted genes. Annotation is based on *M. guttatus* Annotation v2.0, phytozome.net (*M. guttatus* v1.1 assembly scaffolds are separated by dotted lines with double hash marks).

allele resides exclusively within the nearly invariant group 1 haplotype.

But is this pattern of nucleotide diversity at *hms1* unique, or might we find other such low-variation haplotypes throughout the genome? To address this question, we examined genomic variation among the 10 resequenced IM inbred lines (5 with the group 1 haplotype, 5 with group 2), conditioning on two key attributes of the *hms1* haplotype: its genetic size (1.6 cM, estimated from an integrated genetic map fit to physical positions) and allele frequency (50% among the 10 resequenced lines). Centered on SNPs with alleles at 50% frequency (N = 181,659 SNPs), we compared nucleotide diversity in 1.6-cM windows among haplotype groups (defined by alternate alleles at the central SNP). Using this approach, we generated a null expectation for *hms1* diversity:

$$\mathrm{abs}\left[\log_{10}(\pi_1/\pi_2)\right],$$

where π_1 and π_2 is the pairwise diversity in a 1.6-cM block for the five haplotypes associated with allele 1 and the five haplotypes associated with allele 2, respectively. Comparison with this null distribution reveals that the pattern of variation at the *hms1*-associated haplotype is indeed exceptional (Figure 3B).

This pattern is consistent with a strong, partial selective sweep of the group 1 haplotype in the Iron Mountain population (*e.g.*, Voight *et al.* 2006). Assuming typical rates of recombination (one crossover/chromosome), the group 1 haplotype is likely to be young (~63 generations old, for a 1.6-cM block). Its recent origin explains the extreme paucity of variation we observe (<1 mutation expected for 63 generations with mutation rate $\mu = 1 \times 10^{-8}$; observed SNPs ~0, after accounting for sequencing error) (see *Materials and Methods*). How strong would natural selection have to be for the group 1 haplotype to increase in frequency so dramatically over such a short time scale? Population genetic theory predicts that a newly derived allele with a selection coefficient s will take time $t \approx 2\log(2N_e)/s$ generations to reach fixation (note that because the group 1 haplotype is at 44% frequency, the equation provides only a crude approximation). Assuming $t \sim 63$ generations and $N_e \sim 10{,}000$ (a reasonable estimate for the large IM population), the strength of selection should be on the order of 0.15.

Discussion

In recent years, speciation geneticists have made a great deal of progress toward understanding the molecular functions and evolutionary histories of genes involved in hybrid dysfunction. Nevertheless, there is still much to learn about the population genetic forces and selective agents that initially drive substitutions at these genes within species. In this report, we fine map hybrid sterility between two evolutionarily young species of *Mimulus*, narrowing the *hms1* and *hms2* incompatibility loci to small genomic regions with strong candidate genes. We take advantage of polymorphism at *hms1* to investigate the evolutionary dynamics of this locus within a natural population of *M. guttatus*. Our population genomics analyses provide

Table 2 Variation at the *hms1* locus within the Iron Mountain population of *M. guttatus*

	PV *hms1*: GN		PV *hms1*: NN			
IM line	*hms2*: GN	*hms2*: NN	*hms2*: GN	*hms2*: NN	F_{hms1}	$F_{hms1\text{-}2}$
624	0.410 (0.064, 17)	0.535 (0.088, 9)	0.400 (0.088, 9)	0.594 (0.099, 7)	0.081	0.165
617	0.717 (0.055, 6)	0.732 (0.030, 21)	0.819 (0.096, 2)	0.677 (0.034, 16)	0.153	1.724
1189	0.627 (0.078, 10)	0.477 (0.068, 13)	0.528 (0.087, 8)	0.453 (0.078, 10)	0.625	0.235
155	0.751 (0.062, 9)	0.767 (0.066, 8)	0.696 (0.071, 7)	0.708 (0.048, 15)	0.830	0.002
767	0.707 (0.058, 14)	0.615 (0.060, 13)	0.717 (0.062, 12)	0.737 (0.065, 11)	1.188	0.845
323	0.740 (0.076, 7)	0.783 (0.061, 11)	0.600 (0.064, 10)	0.753 (0.082, 6)	1.428	0.602
591	0.486 (0.074, 16)	0.479 (0.085, 12)	0.538 (0.072, 17)	0.669 (0.099, 9)	2.115	0.692
1152	0.722 (0.070, 12)	0.644 (0.085, 8)	0.492 (0.067, 13)	0.638 (0.097, 13)	2.623	2.326
1145	0.287 (0.180, 1)	0.733 (0.052, 12)	0.691 (0.074, 6)	0.677 (0.060, 9)	2.734	4.776
1724	0.502 (0.176, 1)	0.412 (0.049, 13)	0.810 (0.072, 6)	0.761 (0.059, 9)	10.309**	0.040
693	0.556 (0.084, 7)	0.263 (0.111, 4)	0.833 (0.100, 5)	0.703 (0.079, 8)	14.390**	0.740
160	0.537 (0.064, 11)	0.384 (0.061, 12)	0.790 (0.095, 5)	0.780 (0.075, 8)	18.858****	0.912
245	0.605 (0.056, 14)	0.188 (0.075, 8)	0.899 (0.094, 5)	0.720 (0.094, 5)	25.751****	2.144
412	0.661 (0.049, 12)	0.369 (0.070, 6)	0.767 (0.070, 6)	0.886 (0.051, 11)	26.277****	11.546**
62	0.656 (0.062, 10)	0.166 (0.053, 14)	0.685 (0.053, 14)	0.757 (0.053, 14)	31.440****	25.936****
232	0.494 (0.040, 10)	0.528 (0.038, 11)	0.792 (0.048, 7)	0.725 (0.036, 12)	37.182****	1.538
320	0.581 (0.036, 23)	0.252 (0.036, 23)	0.689 (0.052, 11)	0.671 (0.033, 27)	43.818****	15.338**
294	0.704 (0.055, 7)	0.169 (0.042, 12)	0.887 (0.051, 8)	0.784 (0.042, 12)	69.145****	20.179****

Least squared means of pollen viability (PV) for each of four *hms1–hms2* genotypic classes in SF5-backcross progeny using various Iron Mountain (IM) inbred lines (GN = heterozygote and NN = SF5 homozygote). Values in parentheses are standard errors and number of progeny for each genotypic class. The last two columns show results of ANOVAs to test the effect of genotype at *hms1* (F_{hms1}) and of both *hms1* and *hms2* ($F_{hms1\text{-}2}$) on pollen viability. IM lines in boldface type indicate those with whole genome resequence data. $^{**}P < 0.005$, $^{****}P < 0.0001$.

strong evidence that the *hms1* incompatibility allele is involved in a partial selective sweep. Indeed, to our knowledge, we provide the first estimate of the strength of selection acting on a polymorphic hybrid incompatibility allele. Further work will be needed to identify both the underlying cause of selection at *hms1* and the mechanism of interaction between hybrid sterility loci, but this study provides a strong framework for direct investigations of the evolution of hybrid dysfunction.

We have now fine mapped both partners of the *hms1-hms2* incompatibility to small genomic intervals, each with only a handful of genes. Because the incompatibility affects the fertility of both sexes in *Mimulus* hybrids (Sweigart *et al.* 2006), we expect the causal genes to be involved in a process common to both male and female gametogenesis. *Mimulus* species are hermaphroditic and have flowers that contain male and female reproductive structures. In higher plants, the development of both male and female gametes initiates with the differentiation of archisporial cells and meiosis. The meiotic products then undergo two or three rounds of mitosis to produce multicellular gametophytes (the pollen grain and embryo sac). In *Arabidopsis*, a number of meiotic and mitotic cell cycle mutants have been isolated that cause sterility in one or both sexes (Liu and Qu 2008). Intriguingly, both *hms1* and *hms2* contain genes predicted to play key roles in cell cycle regulation.

The *hms1* locus has three strong candidate genes: *Migut.F01605*, *Migut.F01606*, and *Migut.F01612*. The first two are tandem duplicates of *SKP1*-like genes (*M. guttatus* has 13 predicted *SKP1*-like genes genome-wide). Conserved throughout eukaryotes, SKP1 is a subunit of the SKP1–Cullin–F-box protein (SCF) E3 ubiquitin ligase, a complex that regulates diverse developmental processes including the cell cycle (Hellmann and Estelle 2002). In *Arabidopsis* and *Oryza*, this gene family has undergone independent expansions and tandem duplicates are common in both species (Kong *et al.* 2007). Although most of the 21 *Arabidopsis-SKP1*-like (*ASK*) genes have not yet been functionally characterized, mutants in *ASK1* show defects in meiotic chromosome segregation and are male sterile (Yang *et al.* 1999). Interestingly, the other strong candidate for the *hms1* sterility phenotype, an F-box gene, is also a component of the SCF regulatory complex. A key question is whether *hms1* is caused by a single gene or instead by two or more tightly linked genes. In rice, adjacent genes are involved in two different cases of hybrid sterility between the *indica* and *japonica* subspecies (Long *et al.* 2008; Yang *et al.* 2012).

Based on predicted molecular function, only one of the five *hms2* genes is a strong candidate for involvement in *Mimulus* hybrid sterility. The annotation for this gene (*Migut.M00294*) identifies it as related to a cyclin-dependent kinase (CDK) and its top BLAST hit in *Arabidopsis thaliana* encodes a CDK-like (CKL) protein. In *Arabidopsis*, 15 evolutionarily related CKLs were identified as core regulators of the cell cycle by their gene expression profiles (Menges *et al.* 2005). Although there is not yet information on the precise molecular functions of CKLs, they share high sequence similarity with CDKs, which control cell cycle progression in all eukaryotes (Dewitte and Murray 2003). Moreover, *Arabidopsis* mutants for an A-type CDK (*CDKA; 1*) are male sterile due to defects in pollen meiosis II (Nowack *et al.* 2005; Iwakawa *et al.* 2006. Beyond its molecular function, we have discovered a potentially important, *M. nasutus*-specific substitution in *Migut.M00294*: in the third codon of this gene, *M. nasutus* carries a SNP that changes a cysteine to a glycine ($N = 5$ *M. nasutus* lines).

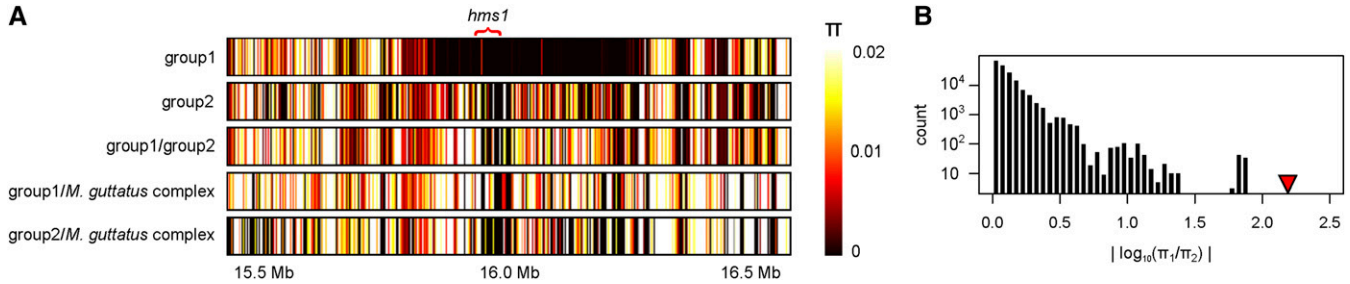

Figure 3 Signature of a selective sweep at the *hms1* locus. (A) Each of the five panels shows nucleotide diversity (π) on linkage group 6 near the *hms1* locus at 1-kb resolution (heat map color scheme is to the right). The *hms1* sterility allele is embedded in a low-variation, 320-kb haplotype (top panel) that appears to have evolved recently in the IM population. Panels are as follows: group 1 = 5 IM lines that carry the 320-kb haplotype associated with hybrid sterility, group 2 = 5 IM lines with typical levels of nucleotide diversity, and *M. guttatus* complex = 10 *M. guttatus* complex lines collected from diverse locales (Table S2). (B) A histogram of the genome-wide distribution of the abs [$\log_{10}(\pi_1/\pi_2)$] test statistic, excluding sites in the 320-kb region. The maximum value of the test statistic from within the 320-kb haplotype (red triangle) is 2.2. Note that this value comes from a site near the center of the low-diversity region.

Although the function of this cysteine is unknown, it is generally conserved among homologous sequences from higher plants (Figure S1) and a change to glycine is predicted to be functionally deleterious (protein variation effect analyzer, PROVEAN score = −7.7; Choi *et al.* 2012). In selfing populations, the efficacy of purifying selection is expected to be reduced due to a drop in effective population size and recombination rates (Nordborg 2000; Charlesworth and Wright 2001). One intriguing possibility is that this Cys-to-Gly mutation has reached high frequency in *M. nasutus* as a consequence of the transition to self-fertilization, as appears to be the case for numerous other putatively deleterious mutations (Brandvain *et al.* 2014). Further experiments will be needed to determine the functional significance of this substitution, but like this *Migut.M00294* glycine variant, previous genetic analyses (Sweigart *et al.* 2007) suggest that the *hms2* incompatibility allele is specific to *M. nasutus*.

Even before getting to the gene level, fine mapping has provided sufficient resolution to begin investigating the evolutionary dynamics of the polymorphic *hms1* locus. Together, the results from our genetic crosses and population genomic analyses suggest that the *hms1* incompatibility allele is associated with a partial selective sweep. The selective advantage of this allele (or one at a tightly linked locus) is apparently substantial ($s \sim 0.15$). In *Drosophila*, most of the hybrid incompatibility genes that have been cloned have also been shown to be rapidly evolving (Ting *et al.* 1998; Presgraves *et al.* 2003; Barbash *et al.* 2006; Brideau *et al.* 2006; Phadnis and Orr 2009; Tang and Presgraves 2009). Similarly, a gene that causes hybrid sterility between mouse subspecies (*Prdm9*) has undergone recurrent bouts of positive selection (Oliver *et al.* 2009). In plants, it is not yet clear how often natural selection is a primary driver of hybrid incompatibilities. In several cases, hybrid dysfunction is caused by divergence at duplicate genes in a manner consistent with the action of random genetic drift (Bikard *et al.* 2009; Mizuta *et al.* 2010; Yamagata *et al.* 2010). On the other hand, it was recently shown that a hybrid lethality allele has risen to high frequency in a population of *M. guttatus* due to linked selection for an allele that confers copper tolerance (Wright *et al.* 2013). Natural selection is also presumed to play a role in divergence among disease resistance genes that cause hybrid necrosis in *Arabidopsis* and rice (Kruger *et al.* 2002; Bomblies *et al.* 2007; Alcazar *et al.* 2009; Jeuken *et al.* 2009; Yamamoto *et al.* 2010; Chen *et al.* 2014), although direct population genetic evidence is lacking. Likewise, the genes that cause cytoplasmic male sterility between *Mimulus* species (involving the same IM62 and SF lines used in this study) seem more likely to have evolved by selfish mitochondrial evolution and compensatory nuclear coevolution than by genetic drift (Barr and Fishman 2010). Adding to these previous studies, our finding that *hms1* is involved in a selective sweep provides some of the strongest evidence to date that natural selection within plant species (in this case, *M. guttatus*) can lead to postzygotic reproductive isolation between species.

The selective sweep at *hms1* raises several additional questions. For one, it is not clear whether *hms1* or a linked gene is the target of selection. Might the *hms1* sterility allele be spreading by genetic hitchhiking as has been seen for *M. guttatus* hybrid lethality and copper tolerance alleles (Wright *et al.* 2013)? Additionally, we do not yet know the underlying cause of natural selection. Is there an ecological advantage of the sweeping *hms1*-associated haplotype? Alternatively, might the *hms1* incompatibility allele provide no direct benefit, but instead evolve selfishly to bias its own transmission? Consistent with this second possibility, we observe non-Mendelian inheritance at *hms1* in certain *M. guttatus–M. nasutus* hybrids (A. L. Sweigart, unpublished data). However, we do not yet know whether transmission ratio distortion at *hms1* also occurs *within* the Iron Mountain population of *M. guttatus*, as has been found for a female meiotic drive locus associated with the LG11 centromere (Fishman and Saunders 2008). Another issue is whether the *hms1* incompatibility allele is on its way to fixation or maintained at an intermediate frequency by short-term balancing selection. With such strong selection and no

counteracting fitness effects, the *hms1* incompatibility allele is expected to spread quickly. Fortunately, we can test this prediction: future field studies at Iron Mountain will measure the fitness effects of alternative *hms1* alleles and track allele frequency changes across years. Finally, is there any evidence that natural selection has also contributed to the spread of the *hms2* incompatibility allele? Demographic effects of selfing (*e.g.*, population bottlenecks) make it challenging to detect selection in *M. nasutus*, but functional experiments to determine allelic effects on fitness may help resolve this issue.

Another question concerns the evolutionary origins of the *hms1-hms2* incompatibility. Did the *hms1* and *hms2* incompatibility alleles arise as new mutations or instead from standing variation? There is evidence that the *hms1* hybrid incompatibility allele is present in other populations near Iron Mountain (Sweigart *et al.* 2007; A. L. Sweigart, unpublished data). One possibility is that this allele was introduced to Iron Mountain through a recent admixture event. As for *hms2*, the incompatibility allele is specific to *M. nasutus* among the samples examined thus far (Sweigart *et al.* 2007). However, it is certainly possible that more intensive sampling will show this allele is also present at low frequency in *M. guttatus*, particularly in the region of California where *M. nasutus* likely originated (Brandvain *et al.* 2014). Given the recent divergence of these *Mimulus* species, this system holds great promise for understanding the evolution of postzygotic reproductive isolation as a continuum, from the initial dynamics within species to the mechanisms of hybrid breakdown between species.

Acknowledgments

We thank John Willis and John Kelly for sharing their Iron Mountain inbred lines. We are grateful to Amanda Kenney for assistance with rQTL. We thank Lila Fishman and Graham Coop for valuable discussions. Lila Fishman, Dave Hall, John Willis, Matt Zuellig, and two anonymous reviewers made thoughtful comments on an earlier draft, which greatly improved the manuscript. We are especially indebted to Rachel Hughes for expert greenhouse care and genotyping assistance. We also thank the Duke Genome Sequencing and Analysis Core, the University of North Carolina Chapel Hill High-Throughput Sequencing Facility, and the Joint Genome Institute for generating the sequences used in this study. This work was supported by National Science Foundation (NSF) grant DEB-1350935 and funds from the University of Georgia Research Foundation to A.L.S., a National Institutes of Health Ruth L. Kirschstein NRSA award (F32GM090763) to L.E.F., and NSF grant DEB-0918902 to Lila Fishman.

Literature Cited

Alcázar, R., A. V. García, J. E. Parker, and M. Reymond, 2009 Incremental steps toward incompatibility revealed by Arabidopsis epistatic interactions modulating salicylic acid pathway activation. Proc. Natl. Acad. Sci. USA 106: 334–339.

Bai, C., P. Sen, K. Hofmann, L. Ma, M. Goebl *et al.*, 1996 SKP1 connects cell cycle regulators to the ubiquitin proteolysis machinery through a novel motif, the F-box. Cell 86: 263–274.

Barbash, D. A., P. Awadalla, and A. M. Tarone, 2006 Functional divergence caused by ancient positive selection of a Drosophila hybrid incompatibility locus. PLoS Biol. 2: e142.

Barkan, A., and I. Small, 2014 Pentatricopeptide repeat proteins in plants. Annu. Rev. Plant Biol. 65: 415–442.

Barr, C. M., and L. Fishman, 2010 The nuclear component of a cytonuclear hybrid incompatibility in *Mimulus* maps to a cluster of pentatricopeptide repeat genes. Genetics 184: 455–465.

Bikard, D., D. Patel, C. L. Metté, V. Giorgi, C. Camilleri *et al.*, 2009 Divergent evolution of duplicate genes leads to genetic incompatibilities within *A. thaliana*. Science 323: 623–626.

Bomblies, K., and D. Weigel, 2007 Hybrid necrosis: autoimmunity as a potential gene-flow barrier in plant species. Nat. Rev. Genet. 8: 382–393.

Bomblies, K., J. Lempe, P. Epple, N. Warthmann, C. Lanz *et al.*, 2007 Autoimmune response as a mechanism for a Dobzhansky-Muller-type incompatibility syndrome in plants. PLoS Biol. 5: e236.

Brandvain, Y., A. M. Kenney, L. Flagel, G. Coop, and A. L. Sweigart, 2014 Speciation and introgression between *Mimulus nasutus* and *Mimulus guttatus*. PLoS Genet. 10: e1004410.

Brideau, N. J., H. A. Flores, J. Wang, S. Maheshwari, X. Wang *et al.*, 2006 Two Dobzhansky-Muller genes interact to cause hybrid lethality in Drosophila. Science 314: 1292–1295.

Broman, K. W., H. Wu, Ś. Sen, and G. A. Churchill, 2003 R/qtl: QTL mapping in experimental crosses. Bioinformatics 19: 889–890.

Canales, C., A. M. Bhatt, R. Scott, and H. Dickinson, 2002 *EXS*, a putative LRR receptor kinase, regulates male germline cell number and tapetal identity and promotes seed development in *Arabidopsis*. Curr. Biol. 12: 1718–1727.

Case, A. L., and J. H. Willis, 2008 Hybrid male sterility in *Mimulus* (Phrymaceae) is associated with a geographically restricted mitochondrial rearrangement. Evolution 62: 1026–1039.

Charlesworth, D., and S. I. Wright, 2001 Breeding systems and genome evolution. Curr. Opin. Genet. Dev. 11: 685–690.

Chen, C., H. Chen, Y. S. Lin, J. B. Shen, J. X. Shan *et al.*, 2014 A two-locus interaction causes interspecific hybrid weakness in rice. Nat. Commun. 5: 3357.

Cheung, W. Y., N. Hubert, and B. S. Landry, 1993 A simple and rapid DNA microextraction method for plant, animal, and insect suitable for RAPD and other PCR analyses. Genome Res. 3: 69–70.

Choi, Y., G. E. Sims, S. Murphy, J. R. Miller, and A. P. Chan, 2012 Predicting the functional effect of amino acid substitutions and indels. PLoS ONE 7: e46688.

Christie, P., and M. R. MacNair, 1987 The distribution of postmating reproductive isolating genes in populations of the yellow monkey flower, *Mimulus guttatus*. Evolution 41: 571–578.

Cutter, A. D., 2012 The polymorphic prelude to Bateson-Dobzhansky-Muller incompatibilities. Trends Ecol. Evol. 27: 209–218.

Darwin, C., 1859 *On the Origin of Species by Means of Natural Selection*. J. Murray, London.

DePristo, M. A., E. Banks, R. Poplin, K. V. Garimella, J. R. Maguire *et al.*, 2011 A framework for variation discovery and genotyping using next-generation DNA sequencing data. Nat. Genet. 5: 491–498.

Devoto, A., M. Nieto-Rostro, D. Xie, C. Ellis, R. Harmston *et al.*, 2002 COI1 links jasmonate signaling and fertility to the SCF ubiquitin-ligase complex in Arabidopsis. Plant J. 32: 457–466.

Dewitte, W., and J. A. Murray, 2003 The plant cell cycle. Annu. Rev. Plant Biol. 54: 235–264.

Diaz, A., and M. R. MacNair, 1999 Pollen tube competition as a mechanism of prezygotic reproductive isolation between *Mimulus nasutus* and its presumed progenitor *M. guttatus*. New Phytol. 144: 471–478.

Diévart, A., and S. E. Clark, 2004 LRR-containing receptors regulating plant development and defense. Development 131: 251–261.

Dobzhansky, T. H., 1937 *Genetics and the Origin of Species*, Columbia University Press, New York.

Drakakaki, G., W. van de Ven, S. Pan, Y. Miao, J. Wang *et al.*, 2012 Isolation and proteomic analysis of the SYP61 compartment reveal its role in exocytic trafficking in Arabidopsis. Cell Res. 22: 413–424.

Fishman, L., and A. Saunders, 2008 Centromere-associated female meiotic drive entails male fitness costs in monkeyflowers. Science 322: 1559–1562.

Fishman, L., A. L. Sweigart, A. M. Kenney, and S. Campbell, 2014 Major quantitative trait loci control divergence in critical photoperiod for flowering between selfing and outcrossing species of monkeyflower (Mimulus). New Phytol. 201: 1498–1507.

Flagel, L. E., J. H. Willis, and T. J. Vision, 2014 The standing pool of genomic structural variation in a natural population of Mimulus guttatus. Genome Biol. Evol. 6: 53–64.

Frank, S. A., 1990 Divergence of meiotic drive-suppression systems as an explanation for sex-biased hybrid sterility and inviability. Evolution 45: 262–267.

Gusti, A., N. Baumberger, M. Nowack, S. Pusch, H. Eisler *et al.*, 2009 The Arabidopsis thaliana F-box protein FBL17 is essential for progression through the second mitosis during pollen development. PLoS ONE 4: e4780.

Hellmann, H., and M. Estelle, 2002 Plant development: regulation by protein degradation. Science 297: 793–797.

Hurst, L. D., and A. Pomiankowski, 1991 Causes of sex ratio bias may account for unisexual sterility in hybrids: a new explanation of Haldane's rule and related phenomena. Genetics 128: 841–858.

Iwakawa, H., A. Shinmyo, and M. Sekine, 2006 Arabidopsis CDKA; 1, a cdc2 homologue, controls proliferation of generative cells in male gametogenesis. Plant J. 45: 819–831.

Jeuken, M. J. W., N. W. Zhang, L. K. McHale, K. Pelgrom, E. Den Boer *et al.*, 2009 Rin4 causes hybrid necrosis and race-specific resistance in an interspecific lettuce hybrid. Plant Cell 21: 3368–3378.

Kim, H. J., S. A. Oh, L. Brownfield, S. H. Hong, H. Ryu *et al.*, 2008 Control of plant germline proliferation by SCFFBL17 degradation of cell cycle inhibitors. Nature 455: 1134–1137.

Kim, O. K., J. H. Jung, and C. M. Park, 2010 An Arabidopsis F-box protein regulates tapetum degeneration and pollen maturation during anther development. Planta 232: 353–366.

Kong, H., L. L. Landherr, M. W. Frohlich, J. Leebens-Mack, H. Ma *et al.*, 2007 Patterns of gene duplication in the plant SKP1 gene family in angiosperms: evidence for multiple mechanisms of rapid gene birth. Plant J. 50: 873–885.

Krüger, J., C. M. Thomas, C. Golstein, M. S. Dixon, M. Smoker *et al.*, 2002 A tomato cysteine protease required for cf-2-dependent disease resistance and suppression of autonecrosis. Science 296: 744–747.

Li, H., and R. Durbin, 2010 Fast and accurate long-read alignment with Burrows-Wheeler transform. Bioinformatics 26: 589–595.

Liu, J., and L. J. Qu, 2008 Meiotic and mitotic cell cycle mutants involved in gametophyte development in Arabidopsis. Mol. Plant 1: 564–574.

Long, Y., L. Zhao, B. Niu, J. Su, H. Wu *et al.*, 2008 Hybrid male sterility in rice controlled by interaction between divergent alleles of two adjacent genes. Proc. Natl. Acad. Sci. USA 105: 18871–18876.

Lynch, M., and A. Force, 2000 The probability of duplicate gene preservation by subfunctionalization. Genetics 154: 459–473.

Maheshwari, S., J. Wang, and D. A. Barbash, 2008 Recurrent positive selection of the Drosophila hybrid incompatibility gene Hmr. Mol. Biol. Evol. 25: 2421–2430.

Maheshwari, S., and D. Barbash, 2011 The genetics of hybrid incompatibilities. Annu. Rev. Genet. 45: 331–355.

Martin, N. H., and J. H. Willis, 2007 Ecological divergence associated with mating system causes nearly complete reproductive isolation between sympatric *Mimulus* species. Evolution 61: 68–82.

Martin, N. H., and J. H. Willis, 2010 Geographical variation in postzygotic isolation and its genetic basis within and between two *Mimulus* species. Philos. Trans. R. Soc. Lond. B Biol. Sci. 365: 2469–2478.

Menges, M., S. M. De Jager, W. Gruissem, and J. A. Murray, 2005 Global analysis of the core cell cycle regulators of Arabidopsis identifies novel genes, reveals multiple and highly specific profiles of expression and provides a coherent model for plant cell cycle control. Plant J. 41: 546–566.

Mizuta, Y., Y. Harushima, and N. Kurata, 2010 Rice pollen hybrid incompatibility caused by reciprocal gene loss of duplicated genes. Proc. Natl. Acad. Sci. USA 107: 20417–20422.

Muller, H. J., 1942 Isolating mechanisms, evolution, and temperature. Biol. Symp. 6: 71–125.

Nordborg, M., 2000 Linkage disequilibrium, gene trees and selfing: an ancestral recombination graph with partial self-fertilization. Genetics 154: 923–929.

Nowack, M. K., P. E. Grini, M. J. Jakoby, M. Lafos, C. Koncz *et al.*, 2005 A positive signal from the fertilization of the egg cell sets off endosperm proliferation in angiosperm embryogenesis. Nat. Genet. 38: 63–67.

Oliver, P. L., L. Goodstadt, J. J. Bayes, Z. Birtle, K. C. Roach *et al.*, 2009 Accelerated evolution of the *Prdm9* speciation gene across diverse metazoan taxa. PLoS Genet. 5: e1000753.

Phadnis, N., and H. A. Orr, 2009 A single gene causes both male sterility and segregation distortion in Drosophila hybrids. Science 323: 376–379.

Presgraves, D. C., 2010 The molecular evolutionary basis of species formation. Nat. Rev. Genet. 11: 175–180.

Presgraves, D. C., L. Balagopalan, S. M. Abmayr, and H. A. Orr, 2003 Adaptive evolution drives divergence of a hybrid inviability gene between two species of Drosophila. Nature 423: 715–719.

Saha, D., A. M. Prasad, and R. Srinivasan, 2007 Pentatricopeptide repeat proteins and their emerging roles in plants. Plant Physiol. Biochem. 45: 521–534.

Sweigart, A. L., and J. H. Willis, 2003 Patterns of nucleotide diversity in two species of *Mimulus* are affected by mating system and asymmetric introgression. Evolution 57: 2490–2506.

Sweigart, A. L., and J. H. Willis, 2012 Molecular evolution and genetics of postzygotic reproductive isolation in plants. F1000 Biol. Rep. 4: 23.

Sweigart, A. L., L. Fishman, and J. H. Willis, 2006 A simple genetic incompatibility causes hybrid male sterility in *Mimulus*. Genetics 172: 2465–2479.

Sweigart, A. L., A. R. Mason, and J. H. Willis, 2007 Natural variation for a hybrid incompatibility between two species of *Mimulus*. Evolution 61: 141–151.

Tang, S., and D. C. Presgraves, 2009 Evolution of the Drosophila nuclear pore complex results in multiple hybrid incompatibilities. Science 323: 779–782.

Tao, Y., D. L. Hartl, and C. C. Laurie, 2001 Sex-ratio segregation distortion associated with reproductive isolation in Drosophila. Proc. Natl. Acad. Sci. USA 98: 13183–13188.

Ting, C. T., S. C. Tsaur, M. L. Wu, and C. I. Wu, 1998 A rapidly evolving homeobox at the site of a hybrid sterility gene. Science 282: 1501–1504.

Van Ooijen, J. W., 2006 JoinMap 4, software for the calculation of genetic linkage maps in experimental populations. Kyazma B. V., Wageningen, The Netherlands.

Vickery, Jr., R. K., 1964 Barriers to gene exchange between members of the *Mimulus guttatus* complex Scrophulariaceae. Evolution 18: 52–69.

Vickery, Jr., R. K., 1978 Case studies in the evolution of species complexes in *Mimulus*. Evol. Biol. 11: 405–507.
Voight, B. F., S. Kudaravalli, X. Wen, and J. K. Pritchard, 2006 A map of recent positive selection in the human genome. PLoS Biol. 4: e72.
Wright, K. M., D. Lloyd, D. B. Lowry, M. R. MacNair, and J. H. Willis, 2013 Indirect evolution of hybrid lethality due to linkage with selected locus in *Mimulus guttatus*. PLoS Biol. 11: 1001497.
Xie, D. X., B. F. Feys, S. James, M. Nieto-Rostro, and J. G. Turner, 1998 COI1: an Arabidopsis gene required for jasmonate-regulated defense and fertility. Science 280: 1091–1094.
Yamagata, Y., E. Yamamoto, K. Aya, K. T. Win, and K. Doi *et al.* 2010 Mitochondrial gene in the nuclear genome induces reproductive barrier in rice. Proc. Natl. Acad. Sci. USA 107: 1494–1499.
Yamamoto, E., T. Takashi, Y. Morinaka, S. Lin, J. Wu *et al.*, 2010 Gain of deleterious function causes an autoimmune response and Bateson-Dobzhansky-Muller incompatibility in rice. Mol. Genet. Genomics 283: 305–315.
Yang, M., Y. Hu, M. Lodhi, W. R. McCombie, and H. Ma, 1999 The Arabidopsis SKP1-LIKE1 gene is essential for male meiosis and may control homologue separation. Proc. Natl. Acad. Sci. USA 96: 11416–11421.
Yang, J., X. Zhao, K. Cheng, H. Du, Y. Ouyang *et al.*, 2012 A killer-protector system regulates both hybrid sterility and segregation distortion in rice. Science 337: 1336–1340.
Zhao, D. Z., G. F. Wang, B. Speal, and H. Ma, 2002 The EXCESS MICROSPOROCYTES1 gene encodes a putative leucine-rich repeat receptor protein kinase that controls somatic and reproductive cell fates in the Arabidopsis anther. Genes Dev. 16: 2021–2031.
Zhao, Z. G., S. S. Zhu, Y. H. Zhang, X. F. Bian, Y. Wang *et al.*, 2010 Molecular analysis of an additional case of hybrid sterility in rice (*Oryza sativa* L.). Planta 233: 485–494.

Communicating editor: L. C. Moyle

GENETICS

Supporting Information
http://www.genetics.org/lookup/suppl/doi:10.1534/genetics.114.171819/-/DC1

Evidence of Natural Selection Acting on a Polymorphic Hybrid Incompatibility Locus in *Mimulus*

Andrea L. Sweigart and Lex E. Flagel

DOI: 10.1534/genetics.114.171819

Table S1 Primer sequences for markers used to fine map *hms1* and *hms2*.

Marker	F primer	R primer	Target locus	RE
25998	CGTCTACTCAAGAAAACGACGA	GGTAATTGGCTGCATTACCAA	*hms1*	
M8	GGTGGCCATTTCTACACCAT	CCAACTGCATCCACATCATC	*hms1*	
M24	ATCCACAGCTTGAGGTGGTC	CACACAGACAACTCGCTCGT	*hms1*	
M119	TGTTGTTGCGAAGAAAGCTG	CCGTTTCCGTCTTCATCATT	*hms1*	
M120	GTCGCCGTTATTCTCCTCCT	CCTCTCCAGAAACCAACCAC	*hms1*	
seq01	ACACCTTAACACGGCCTCTC	CGAAAGATGGGCTTTGAATC	*hms1*	
seq02	GCAACACAAGGACAAGCATC	GACTCCGTTTCGGAAAAATG	*hms1*	
seq14	CGCGTAAATTTCGTATTGCAT	CGCGTGCGGAAAAACTAC	*hms1*	
seq15	TTTGCTTCGAAGAATTCAATG	CGGAAGCCAATAGCTCGAT	*hms1*	
seq26	ACACCTCGAAAAATCCAACG	CTAGCGAGCCATTGGTTGAT	*hms1*	
seq27	GACGAGGGTAAACCGGTAAAA	TCGTGTACCGAGCAATTCAG	*hms1*	
seq31	CCAGAAAAATTGCTGCTTGA	GAAGACATATGCTCCAATTCTGG	*hms1*	
seq32	TCCCCTGAGCTATTTCTCCA	CCCTAACGGAATGAATGAGTTG	*hms1*	
seq34	GTACAACACCCGAACCTCGT	AGTCGAAGAAGCAAGCATGG	*hms1*	
hms1CAPS1	TAAAAGCCTCCGAAATCCAA	TGGAAGCAAACAATAAAACGAA	*hms1*	SacI
hms1CAPS2	ACGAGCAGACATTCGCTTCT	TCCGCCAAACCACTTTATTC	*hms1*	HpaII

M23	CAGCTTCTCGCCTATGGACT	ACAGTGTTTCCACCGCACTC	*hms2*
M33	AGTCCTTCCGGCAAGAGG	CTTCCGGCTATAGGTTGCTG	*hms2*
M51	GCCTTCTGCCTCTTCTTGC	GCCAATACGATTTTCCGTCT	*hms2*
M54	CGTGCGACACGTATTTCTTC	CTTTCCCACAATTTTACGAGAT	*hms2*
M122	GACGGCCAGAATTTAATCCA	TCTCACTCGAGTCCGTTTCA	*hms2*
M211	TCAGAAACCCTATTCGAAATTGA	AGAATCACCAATCCGCAGAG	*hms2*
M216	GAGTTCGCCCTCAAGAGTTG	TCCTCTCCCAGACGAAAAGA	*hms2*
M219	TTACGTGGCCGAAGTTAGGT	CGAATGTACTGTCCCGAGGT	*hms2*
M222	AATGCATTATGGGGAAGGTG	TGGCCGTTGTACATTGTCTC	*hms2*
M262	CTTGAAAAGCTCGGCGTTATC	AAACAGGCACGTGGATGTG	*hms2*

Table S2 Plant lines with whole genome resequence data used in population genomic analysis.

Line	Figure 3 ID	US State of Origin	NCBI Accession #
IM109	Iron Mountain, group 2	OR	SRX021073
IM1145	Iron Mountain, group 2	OR	SRX021074
IM155	Iron Mountain, group 2	OR	SRX055301
IM320	Iron Mountain, group 1	OR	SRX055300
IM479	Iron Mountain , group 1	OR	SRX021077
IM62	Iron Mountain, group 1	OR	SRX021072
IM624	Iron Mountain, group 2	OR	SRX021075
IM693	Iron Mountain, group 1	OR	SRX021078
IM767	Iron Mountain, group 2	OR	SRX021079
IM835	Iron Mountain, group 1	OR	SRX021076
AHQT1.2	*M. guttatus* complex	WY	SRX142379
BOG10	*M. guttatus* complex	NV	SRX030570
DUN	*M. guttatus* complex	OR	SRX030973, SRX030974
LMC24	*M. guttatus* complex	CA	SRX030680
MAR3	*M. guttatus* complex	OR	SRX030542
MED84	*M. guttatus* complex	CA	SRX552649

SF5	*M. guttatus* complex	OR	SRX116529
SLP19	*M. guttatus* complex	CA	SRX142377
SWB-S3-1-8	*M. guttatus* complex	CA	SRX030679
YJS6	*M. guttatus* complex	ID	SRX030545

Table S3 Results from additional progeny testing for a subset of *hms1* recombinants.

Individual	*hms1*		*hms2*	cross	PV *hms2*: NN			F_{hms1}
					segregating *hms1* flanking marker:			
	M8	M24			GG	GN	NN	
39_35	**GN**	NN	NN	SF5	n/a	0.203 (0.022, 17)	0.846 (0.035, 7)	240.446****
20_56	**GN**	NN	NN	self	0.870 (0.042, 6)	0.853 (0.029, 13)	0.873 (0.052, 5)	0.087
29_56	**GN**	NN	NN	self	0.923 (0.035, 7)	0.891 (0.031, 9)	0.812 (0.032, 8)	3.014
27_39	**GN**	NN	NN	self	0.679 (0.176, 3)	0.767 (0.176, 5)	0.622 (0.152, 4)	0.195
30_51	**GN**	NN	NN	self	0.930 (0.023, 4)	0.919 (0.015, 10)	0.846 (0.021, 5)	5.074*
10_46[1]	**GN**	NN	NN	self	0.786 (0.028, 24)	0.810 (.019, 57)	0.812 (0.028, 25)	0.280
20_76	**GN**	NN	NN	self	0.510 (0.058, 20)	0.563 (0.042, 37)	0.639 (0.042, 37)	1.865
47_18	NN	**GN**	NN	self	0.464 (0.254, 1)	0.736 (0.080, 10)	0.513 (0.179, 2)	1.037
15_49[1]	NN	**GN**	NN	self	0.760 (0.778, 6)	0.742 (0.034, 32)	0.831 (0.072, 7)	0.626
25_77[1]	NN	**GN**	NN	self	—	0.825 (0.020, 33)	0.757 (0.036, 10)	2.667

Least squared means of pollen viability (PV) for each of three genotypic classes in *hms1* recombinant selfed or SF5-backcross progeny. All recombinant individuals are heterozygous (GN) at one *hms1* flanking marker (bolded, M8 or M24) and homozygous for SF5 alleles (NN) at the other. At *hms2*, all individuals are NN (*i.e.*, they are NN at both flanking markers M51 and e193). Values in parentheses are standard errors and numbers of progeny for each genotypic class. Recombinants that are NN at the causal *hms1* locus are expected to produce only fertile progeny and the segregating *hms1* flanking marker should show no effect on pollen viability. In contrast, recombinants that are GN at the causal *hms1* locus are expected to segregate for pollen fertility, which should be affected by genotype at the heterozygous flanking marker (*i.e.*, progeny that are GG or GN at the flanking marker should be highly sterile). The last column shows results of an ANOVA to test the effect of genotype at the segregating *hms1* marker (F_{hms1}). Only one of these recombinant individuals (39_35) produces sterile progeny; as expected, pollen viability in these progeny is associated with genotype at *hms1*. Note that certain genotypic classes are missing, either because the cross did not produce them (marked as "n/a") or due to transmission ratio distortion (marked as "—").

[1]Recombinant was originally GG/GN at *hms1* flanking markers; the genotype shown here was generated by a cross to SF5, which represented an initial round of progeny testing to determine whether *hms1* was homozygous for IM62 alleles or heterozygous (see Methods).

* $P<0.05$, **** $P<0.0001$.

Table S4 Results from additional progeny testing for a subset of *hms2* recombinants.

Individual	*hms1*	*hms2*		cross	PV *hms1*: GG			PV *hms1*: GN		
					segregating *hms2* flanking marker:			segregating *hms2* flanking marker:		
		M51	e193		GG	GN	NN	GG	GN	NN
02_66	GN	**GN**	NN	self	0.008 (0.019, 9)	0.006 (0.017, 11)	—	0.255 (0.033, 3)	0.153 (0.020, 8)	0.158 (0.041, 2)
27_62	GN	**GN**	NN	self	0.814 (0.060, 8)	0.501 (0.070, 6)	0.002 (0.121, 2)	0.876 (0.057, 9)	0.649 (0.033, 26)	0.256 (0.099, 3)
38_13	GG	**GN**	NN	self	0.587 (0.032, 34)[1]	0.348 (0.055, 12)	—	n/a	n/a	n/a
31_07	GN	**GN**	NN	self	0.727 (0.035, 17)[1]	0.531 (0.076, 4)	0 (0.152, 1)	0.858, 0.062, 6)	0.638 (0.068, 5)	0.140 (0.076, 4)
19_09	GN	**GN**	NN	self	—	—	—	0.662 (0.040, 11)	0.839 (0.038, 12)	0.072 (0.060, 5)
20_77	GG	**GN**	NN	self	0.709 (0.049, 16)	0.410 (0.038, 26)	0 (0.097, 4)	n/a	n/a	n/a
02_41	GN	NN	**GN**	self	0.407 (0.146, 2)	0.260 (0.167, 2)	0.004 (0.118, 3)	0.581 (0.118, 6)	0.163, 0.118, 5)	0.044 (0.084, 4)
14_46	GN	NN	**GN**	self	—	—	—	—	0.804 (0.164, 1)	0 (0.164, 1)
15_25	GN	NN	**GN**	self	0.902 (0.205, 2)	0.491 (0.205, 2)	0.021 (0.205, 2)	0.745 (0.102, 8)	0.559 (0.092, 10)	0.347 (0.096, 9)
48_81	GN	NN	**GN**	self	0.565 (0.050, 14)[1]	0.597 (0.062, 10)	0.050 (0.107, 3)	0.845 (0.070, 8)	0.808 (0.066, 8)	0.088 (0.076, 6)
34_37	GN	NN	**GN**	SF5	—	—	—	—	0.620 (0.071, 9)	0.113 (0.080, 7)
36_67	GN	NN	**GN**	self	0.447 (0.121, 4)	0.567 (0.121, 8)	0.088 (0.172, 2)	0.752 (0.073, 11)	0.605 (0.052, 22)	0.149 (0.092, 7)

Least squared means of pollen viability (PV) for six genotypic classes in *hms2* recombinant selfed progeny. All recombinant individuals are heterozygous (GN) at one *hms2* flanking marker (bolded, M51 or e193) and homozygous for SF5 alleles (NN) at the other. At *hms1*, these same individuals are heterozygous (GN) or homozygous for IM62 alleles (GG) both flanking markers M8 and M24 (*i.e.*, they are not recombinant in the *hms1* interval). Values in parentheses are standard errors and numbers of progeny for each genotypic class. Selfed progeny of *hms2* recombinants that are NN at the causal *hms2* locus are expected to be highly sterile if they also inherit at least one G allele at *hms1*; among such progeny, the segregating *hms2* flanking marker will have no effect on pollen viability. In contrast, selfed progeny from *hms2* recombinants that are GN at the causal *hms2* locus will segregate for pollen viability (even in a GG or GN *hms1* background) and be affected by genotype at the segregating flanking marker (progeny that carry NN genotypes at the flanking marker are expected to show lower pollen viability than those carrying GG or GN). Only one of these *hms2* recombinant individuals (02_66) produces uniformly sterile progeny in a GG or GN *hms1* background, indicating it is NN at the causal *hms2* locus. All other *hms2* recombinant selfed progeny segregate for pollen viability in a GG or GN *hms1* background, indicating that their parents were heterozygous at *hms2*. For simplicity, only the six most relevant genotypic classes are shown. Note that certain genotypic classes are missing, either because the cross did not produce them (marked as "n/a") or due to transmission ratio distortion (marked as "—").

[1]Genotypic class is enriched because multiple generations of progeny tests were performed; some rounds used individuals that were GG at *hms1* and at one of the *hms2* flanking markers (these individuals were generated by the first round of progeny testing).

PLANT CKL PROTEIN N-TERMINUS MULTIPLE SEQUENCE ALIGNMENT

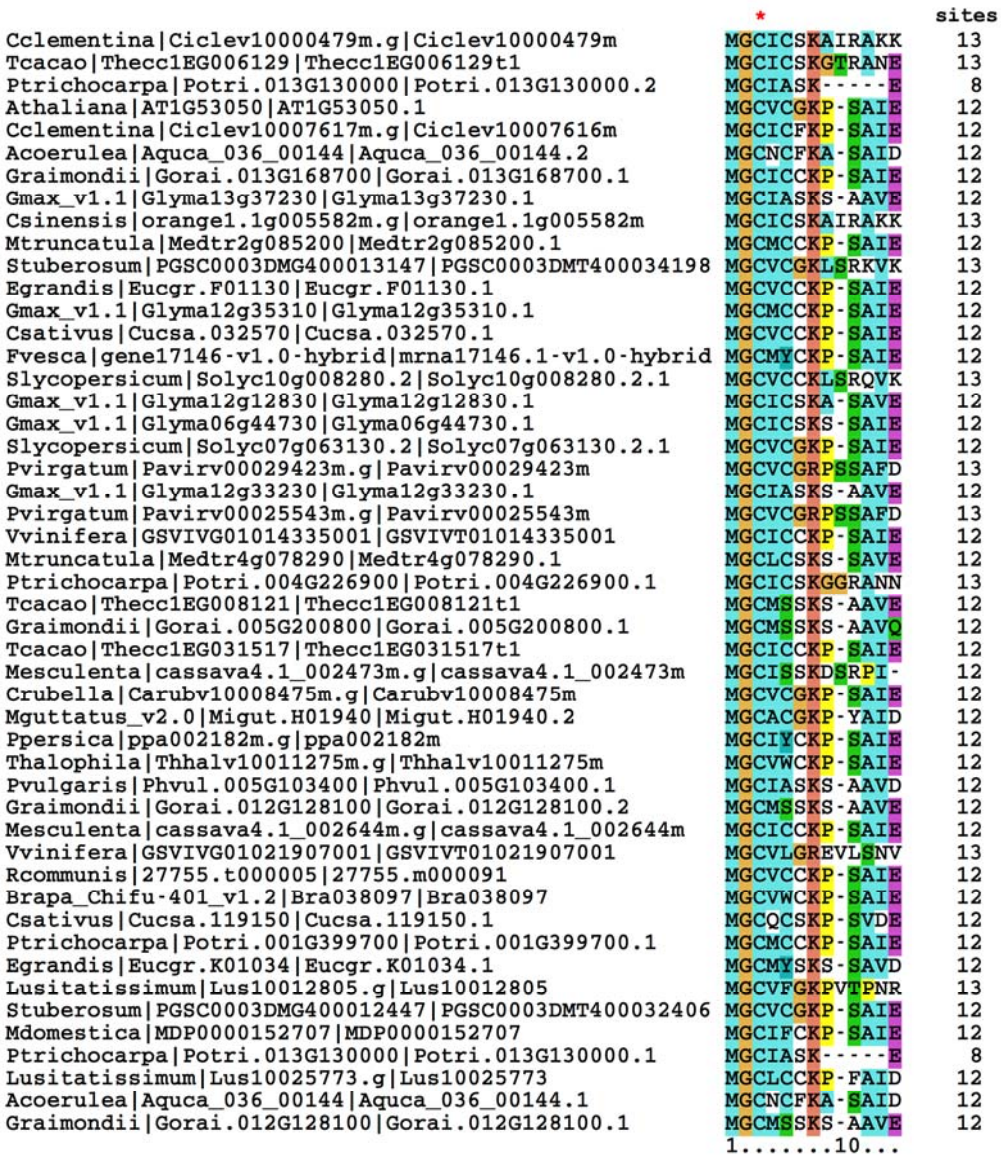

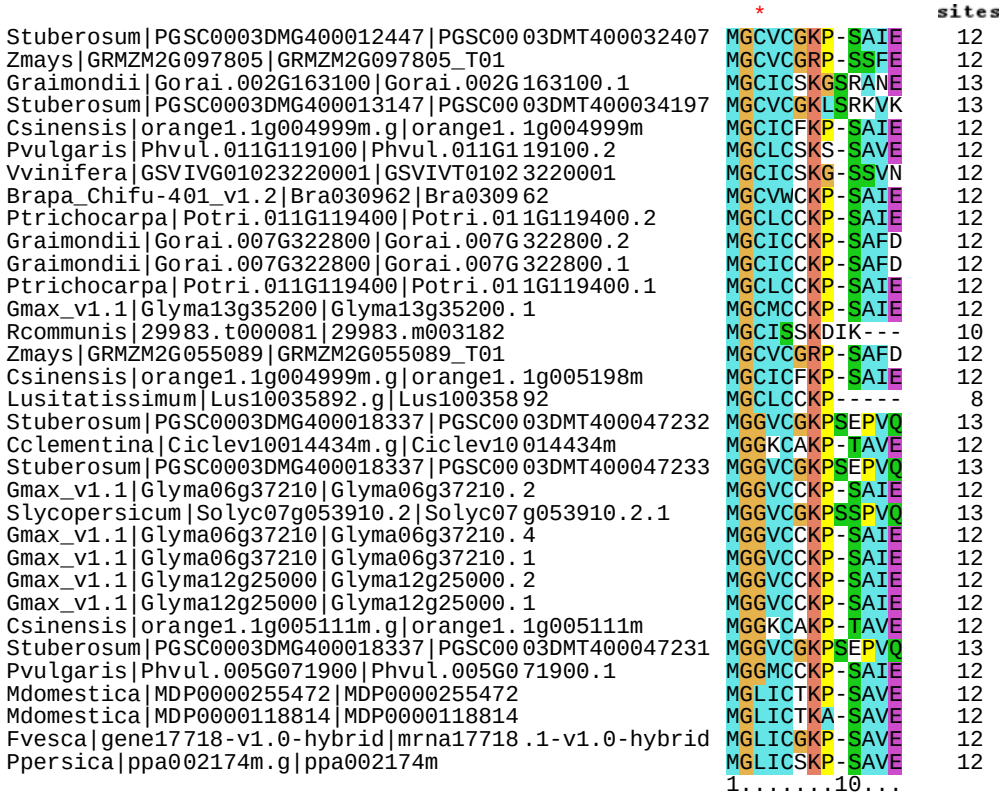

Figure S1 Multiple sequence alignment of plant CKL proteins. Species and gene name are given for each sequence along with the first 13 amino acids of the alignment. The site of the putatively deleterious Cys to Gly polymorphism found between *M. guttatus* and *M. nasutus* is marked with an asterisk. Note that for five species, at least one paralog carries a Gly at this third amino acid position. All sequences retrieved from Phytozome v9.1 (www.phytozome.net) and correspond to cluster ID 38180041.